# Effect of ambient pressure on the internal atomization processes of a gas-turbine fuel injector

K. P. Shanmugadas*[1], E. S. Manuprasad[2], Chiranthan R. Narasimha[3], S. R. Chakravarthy[2]
[1] Department of Mechanical Engineering, Indian Institute of Technology Jammu, India
[2]Department of Aerospace Engineering, and National Centre for Combustion Research and Development, Indian Institute of Technology Madras, Chennai, India.
[3] GE India Industrial Pvt. Ltd., Bengaluru, India
*Corresponding author email : shanmugadas.kp@iitjammu.ac.in

**Abstract**
The present work investigates the internal atomization characteristics of a gas-turbine fuel injector under elevated ambient pressure conditions. The injector is a piloted prefilming type airblast atomizer in which a dual orifice nozzle is used as the pilot nozzle. The injector assembly involves primary and secondary swirlers which are separated by a curved prefilmer called venturi. The fuel placement and droplet size at the injector exit depends on the flow evolution within the atomizer geometry which is influenced by the individual hardware components and ambient conditions. The injector geometry is split into different modules such as pilot nozzle, primary swirler, venturi, secondary swirler etc. and the modules are combined together forming different stages such that spray formation can be tracked as the flow evolves through it. High-speed imaging and laser induced fluorescence (planar and volumetric) imaging are performed to capture the internal flow field and phase Doppler interferometry measurements are conducted to obtain droplet size and axial velocity variation at every stage. Experiments are conducted up to 7 bar ambient pressure at constant fuel air ratio (FAR) with each stage configurations. The increase in ambient pressure lead to the collapse of the primary spray from the dual orifice nozzle which resulted in a narrow cone angle and in the formation of bigger droplets. Further, the ambient pressure influenced the wall filming process forming thick liquid films and rims at the prefilmer tip. The counter-rotating shear layer formed at the secondary swirler exit limited the influence of ambient pressure at the secondary exit and overall, the average droplet size increased at the injector exit. The effect of spray cone collapse of the pilot nozzle spray is not visible at the injector exit. This suggests that the wall filming on the venturi surface and the shear layers at the secondary exit, are the major contributing parameters in the drop formation and fuel placement at the injector exit at elevated pressure operating conditions.

**Keywords**
Swirl cup, laser induced fluorescence imaging, gas-turbine fuel injector.

## Introduction

Swirl cup is considered as one of the efficient airblast injector designs, which is adopted in many of the currently operating rich-burn aero engines [1]. A pilot nozzle, typically a dual orifice type, along with a counter–rotating swirler assembly separated by a curved prefilmer venturi constitute the swirl cup injector assembly (shown in Figure 1). The dual orifice nozzle is used for the fuel staging, based on the engine cycle conditions and power requirements [2]. During the light-up and low power cycle conditions, the central circuit of the dual orifice nozzle alone operates and forms a hollow cone spray. At high power operating conditions, the secondary flow circuit opens forming a wide annular spray in addition to the central spray, and supplies the additional fuel needed for the combustor operation. Droplet size distribution and fuel placement at the injector exit are dictated by the two-phase flow evolution within the

injector [3, 4]. The pilot nozzle spray characteristics and the aerodynamics associated with the air swirl dictate the internal fuel placement and atomization process in the swirl cup. Furthermore, the operating conditions of the combustor such as ambient pressure (P3) and air inlet temperature (T3) influence the internal two-phase flow of the swirl cup and successive atomization processes at the exit.

The effect of ambient pressure and temperature on the spray structure of the pressure swirl and airblast sprays has been investigated in several previous studies [5-12]. In most of these investigations, the external spray structure and drop size variation are captured at various operating conditions. In the case of pressure swirl atomizers and low shear airblast injectors, the average SMD is increased upto a critical pressure range with respect to the rise in ambient pressure. In the case of piloted prefilming type and high shear injectors, the pressure dependence on the droplet size is not clearly understood. The droplet size variation and fuel placement in a practical gas turbine fuel injector like swirl cup, depend on the complex two-phase flow field inside the injector. The internal atomization processes such as atomization of the primary spray, spray-wall interaction, wall filming, rim and film breakup etc. are affected by the changes in air density and velocity variation. The role of inlet air temperature on the spray formation is more straightforward and in most of the cases the drop sizes are reduced by the high evaporation rates at high-temperature conditions. However, the effect of ambient temperature on the individual flow processes varies based on the operating conditions. Hence, it is important to conduct comprehensive investigations to develop a detailed physical understanding of the internal atomization mechanisms of gas turbine fuel injectors at realistic operating conditions.

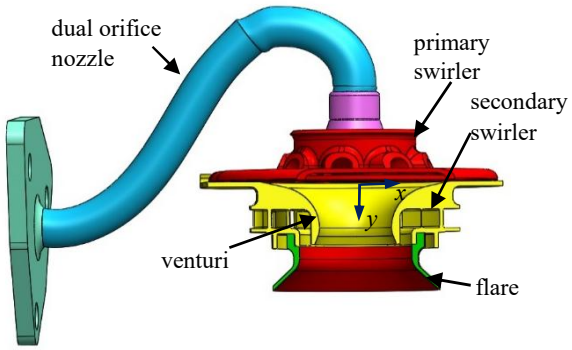


**Figure 1.** Geometry of the swirl cup – nozzle assembly.

Considering the specific case of swirl cup injector, it is reported that poor atomization characteristics are responsible for the higher levels of smoke and soot formation at high power operating conditions [1]. Engineers suspect that the improper impingement of the primary spray on the venturi surface and poor wall filming lead to the formation of bigger droplets which eventually results in improper mixing and incomplete combustion. Hence, it is really important to understand the two-phase flow inside the swirl cup at realistic operating conditions.

The primary objective of the present work is to capture the spray formation inside the swirl cup at elevated ambient pressure conditions. The effect of ambient pressure on the internal atomization processes and their relative dominance on the droplet formation and fuel placement are investigated. Furthermore, it is also aimed to build-up a comprehensive understanding towards improving the fuel injector designs for aero gas turbine engines.

**Experimental Arrangements**

The complex atomizer geometry of the swirl cup poses significant challenges to access the internal flow field for laser diagnostics. A stage-wise characterization approach is adopted to track the spray formation systematically starting from the pilot nozzle to the cup exit. The swirl cup is split into different atomizer components and combined to form different modules as listed below.

1. Case 1: Pilot nozzle alone
2. Case 2: Nozzle + primary swirler
3. Case 3: Nozzle + primary swirler+ venturi
4. Case 4: Nozzle + primary swirler+ venturi + secondary swirler
5. Case 5: Full swirl cup

Spray flow field at the exit in each of the above Cases are captured adopting different laser diagnostic techniques. Details of the stage-wise approach and geometrical combinations are explained in detail in [3]. The prefilmer- venturi is manufactured in toughened glass with a thickness of 0.7 mm maintaining the geometrical features of the actual hardware. This transparent venturi provides the necessary optical access to capture the wall filming and spray impingement inside.

A high pressure-temperature spray test rig is developed to simulate realistic operating conditions. The rig involves a high-pressure chamber with a 5 window optical access which is suitable for performing various laser diagnostics experiments. Details of the test facility and measurement capabilities can be found in [13].

**Test conditions**

In many of the previous investigations [5-9], the effect of ambient pressure (P3) is investigated keeping the air to liquid ratio (ALR) constant, but the air and liquid flow rates are proportionately increased with respect to the change in P3. Even though this represents a typical engine flow scenario, individual effects of ambient conditions need to be investigated. In the present work, the specific effect of ambient pressure is investigated keeping all other operating parameters constant. The behavior of the swirl cup spray to the change in P3 is investigated over a range of 1-7 bar. All other operating parameters such as liquid flow rate, air flow rate, ALR and inlet air temperature, are held constant. The liquid flow rate is 8.3 g/s and the corresponding ALR is 8.7. The overall pressure drop across the swirl cup is maintained at ~3.8 %. For each P3 value, the spray flow field produced by all the five configurations (Cases) is captured. Detailed test conditions are listed in Table 1. Experiments with Case 2 and 3 configurations consider only the primary swirler airflow which is around 40 % of the total mass flow rate through the swirl cup. Based on the ambient density and inlet air temperature ranges, the present test cases represent scaled-down versions of some of the idle and cruising operating conditions of the rich dome aero engines. However, water is taken as the working fluid instead of Jet A considering the difficulties in fluorescence imaging (requirement of UV high speed lasers for exciting Jet A, and quartz venturi parts to transmit the florescence signals), auto ignition risks inside the test chamber, safety issues related to collection and disposal of fuel etc. Atomization processes and overall flow evolution will be similar but the higher evaporation rates of Jet A may produce smaller drops and thinner films.

**Diagnostics**

Time-resolved laser induced fluorescence imaging (TR-LIF) technique is adopted to capture the spray formation inside the swirl cup. Planar LIF imaging (TR-PLIF) experiments are conducted to capture the spray structure with Case 1, 2 and 5 configurations. Volumetric LIF imaging (TR-VLIF) is adopted to capture the wall filming and flow field inside the swirl cup using the Case 3 and 4 configurations. LIF signals only shows the regions where liquid is

present and the laser light reflections from metal/glass surfaces and other multiple scattering effects are avoided. Hence, LIF imaging is adopted instead of direct light sheet imaging. A double-pulsed high-speed Nd:YLF laser (Litron) with a wavelength of 527 nm is used to illuminate the flow field in PLIF imaging. A light sheet optics set (LaVision) is used to convert the laser beam into a thin light sheet of ~1 mm thickness, and the mid-plane (x-y plane) of the injector is illuminated. The desired illumination plane is around 80 mm × 80 mm within which the spatial divergence of the laser sheet intensity is minimal. A high-speed camera (Photron SA5) is synchronized with the laser using a high- speed controller unit, and images are acquired at 5 kHz. A 556 nm narrow bandpass filter attached to the camera is used to collect the LIF signals emitted from Rhodamine 6G dye- water mixture. Data is captured using commercial software (Davis™) from LaVision. The laser beam is made into a cuboidal laser beam of 100 mm × 100 mm cross-section using a volume optics module. This illuminates the entire inside region of the venturi and swirl cup. The optical arrangements with respect to each of the imaging configurations are explained in detail in [3].

**Table 1.** Test conditions.

| ALR | P3 (abs) bar | T3 (K) | $\rho\ (Kg/m^3)$ | $U_{avg}(\ m/s)$ | Re |
|---|---|---|---|---|---|
| 8.7 | 1 | 453 | 0.77 | 74.7 | 90956 |
| | 3 | 453 | 2.31 | 24.9 | 90920 |
| | 5 | 453 | 3.85 | 14.9 | 90848 |
| | 7 | 453 | 5.38 | 10.7 | 90812 |

A three-component phase Doppler interferometry (PDI) instrument from Artium is used to measure the droplet size and axial velocity variation of the spray. Measurements are done at different x/d locations from the exit plane of each Case where spherical droplets are formed. Here, d is the venturi exit diameter. PDI experiments under high-pressure conditions are quite complicated and involve elaborate prior arrangements. Setting up of PDI involves the positioning of the laser beams at the measurement location such that individual beam pairs exactly meet at the same measurement volume. The beams have to pass through the thick glass windows and the beam refraction varies based on the wavelength and angle of incidence. Special fixtures are positioned in the chamber and the beam alignment is performed carefully using a microscope objective. The receiver is also focused through the glass windows. Based on trial experiments, the refractive index is corrected in the PDI software to account the effect of thick glass windows.

Furthermore, PDI measurements also face challenges related to the dense spray conditions and glass window fogging. The dense spray causes the attenuation of the laser beams and poor signal to noise ratios. To alleviate the measurement difficulties associated with the dense spray, test conditions are chosen corresponding to the relatively sparse spray conditions to the extent possible. Further, even a slight window fogging affects the refractive index and over predicts the diameter. Hence, measurements are taken when the windows are clear and sufficient time interval is given between each measurement to allow the evaporation of the droplets that are stick on the windows. Measurements are repeated until sufficient statistics ~ 20000 samples are taken with validation rates above 75 %. The uncertainty in the SMD measurements is < 6 μm and the same in the axial velocity measurements is around ±2%.

## Results

### Effect of ambient pressure on the pilot nozzle spray

The effect of ambient pressure on the pilot nozzle spray structure is characterized initially, following the test matrix given in Table 1. The central nozzle spray is discharged into a quiescent environment maintained at different ambient pressures. Instantaneous PLIF images of the central spray at P3 = 1 bar and 7 bar are shown in Figure 2. At P3= 1 bar, the liquid spray forms a hollow cone spray with an average cone angle of ~ 40°. As the pressure increases, the spray cone collapses and a partially solid cone structure is formed. At P3= 7 bar, the average cone angle is reduced to ~20° and bigger droplets are observed. The increase in chamber pressure results in a corresponding rise in ambient air density, from 0.77 to 5.38 kg/m3. For the same liquid flow rates, the higher aerodynamic resistance opposes the radial expansion of spray and droplet penetration, which eventually causes the spray cone to collapse with a reduction in the cone angle. The amount of air available within the spray cone is limited and the relative velocity is also dropped, leading to poor atomization. Furthermore, a change in the atomization mechanism is also noted at higher pressures. At P3= 1 bar, the spray cone undergoes a perforated sheet breakup forming finer droplets whereas at higher pressures, a wavy sheet breakup occurs forming thick ligaments near the nozzle exit.

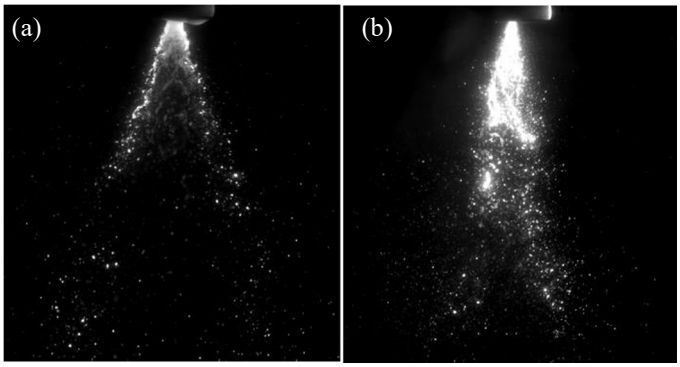


**Figure 2.** Pilot nozzle spray structure at (a) P3 = 1 bar, (b) P3 = 7 bar.

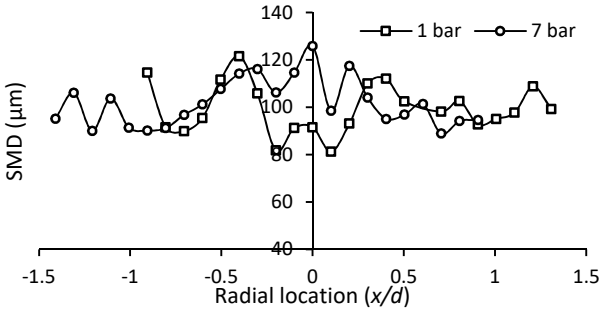


**Figure 3.** Diameter variation of the pilot nozzle spray at P3 = 1 bar and P3= 7 bar (*y/d* = 0.9).

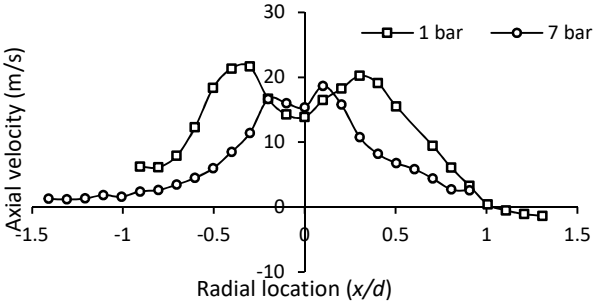


**Figure 4.** Axial velocity variation of the pilot nozzle spray at P3 = 1 bar and P3= 7 bar (*y/d* = 0.9).

The droplet size variation (Figure 3) shows that within the spray cone (-0.5≤ x/d ≤0.5) the SMD is increased at P3 = 7 bar along with a reduction in the axial velocity (Figure 4). In the central region, the peak values of SMD are in the range of 81-114 μm at 1 bar and 106-120 μm at 7 bar. The change in the pilot nozzle spray structure affects the successive atomization processes inside the swirl cup.

**Role of primary air swirl on the pilot nozzle spray**

The primary air flow undergoes a vortex breakdown and forms a central toridal recirculation zone (CTRZ). The pilot nozzle spray is atomized by the primary air swirl and forms a primary spray. The droplets from the pilot nozzle are dispersed into the CTRZ and the relative momentum exchange between the liquid and gas phases dictate the droplet dispersion and fuel placement [13, 14]. The response of the primary spray to the change in ambient pressure is investigated with the Case 2 configuration. Instantaneous PLIF images showing the spray structure at 1 and 7 bar ambient pressures are presented in Figure 5. The narrow cone angle of the pilot nozzle spray directs most of the droplets into the CTRZ. The radial pressure gradients of the CTRZ expands the spray cone which is clearly visible at P3=1 bar. The recirculating air flow promotes entrainment of the smaller drops to the central region while most of the bigger drops aligned to the spray shear layer as the flow proceeds downstream. As P3 increases, the collapse of the primary spray cone is evident even in the presence of primary air and a narrow spray cone is formed with a small recirculation zone at the centre. The cone angle decreases gradually from 55° at 1 bar to 26 °at 7 bar. At higher ambient pressures, the centrifugal forces associated with the CTRZ is opposed by the aerodynamic resistance because of the increase in ambient air density. This limits the radial expansion of the spray at higher pressures.

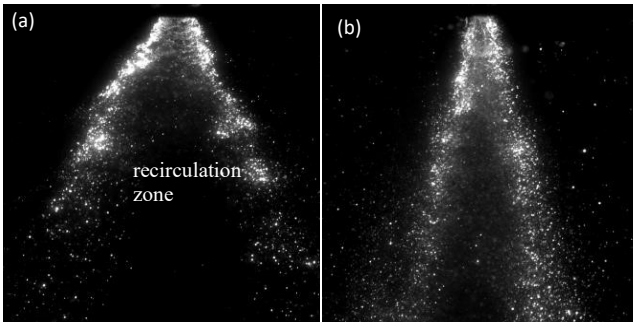


**Figure 5.** Primary spray structure at (a) P3 = 1 bar, (b) P3 = 7 bar.

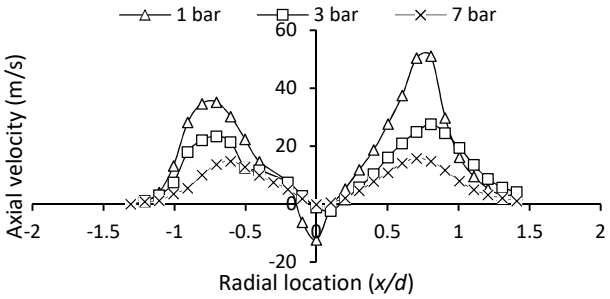


**Figure 6**. Axial velocity variation of the primary spray (y/d = 0.9).

The velocity and droplet size variation at different P3 values are shown in Figures 6 and 7. The droplet axial velocities show a systematic reduction as P3 increases. The rise in the air density with respect to P3, decreases the air velocity for a fixed mass flow rate, and eventually, the lower relative velocity between the primary air and pilot spray droplets affects the

atomization. The diameter variation curves also show an increase in SMD within the spray cone region, as the ambient pressure increases.

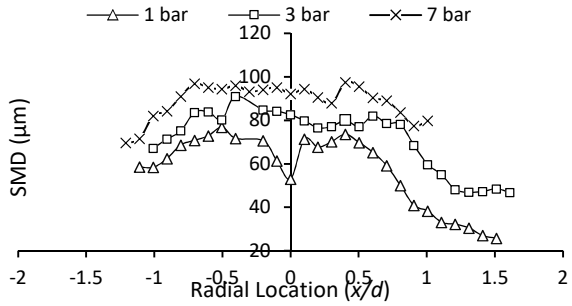


**Figure 7.** Diameter variation of the primary spray (*y/d* = 0.9).

**Effect of ambient pressure on the wall filming**

The role of P3 on wall filming is investigated using the Case 3 configuration in which the secondary air flow is not involved. The purpose of the venturi is to act as the prefilming surface on which the primary spray impinge and forms a thin liquid film. In our previous works [3, 4] and in other recent investigations [15, 16], it is reported that the thickness of accumulated liquid rim is the major deciding factor on the external drop size distribution and not the liquid film thickness. Hence, it is important to understand the film transport and accumulation mechanisms at the venturi tip at realistic conditions.

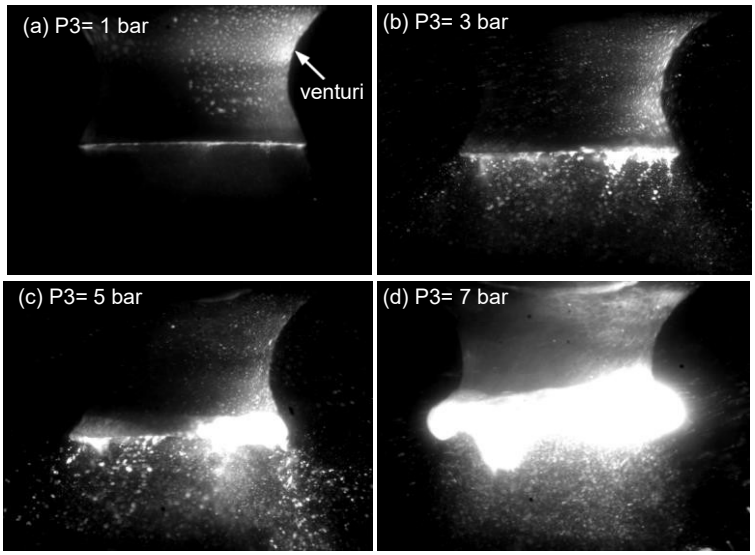


**Figure 8.** Wall filming and rim formation inside the venturi.

TR-VLIF imaging of the venturi flow field offered very interesting results. Instantaneous VLIF images at different P3 values are shown in Figure 8. At P3 = 1 bar, the spray at the venturi exit is very fine, and there is little wall filming on the venturi. The presence of the venturi confines the spray shear layer and CTRZ elongates to further downstream, Most of the well atomized droplets are issued through the central region undergoing secondary atomization as it interacts with primary air swirl. The part of the spray that impinges on the venturi results in wall filming and forms a thinner rim at the venturi tip. As the chamber pressure increases, the spray cone is expanded and most of the primary spray impinges on the venturi wall. This leads to a significant wall-filming and the film accumulates into a thick liquid rim at the venturi tip as shown in Figure 8d. According to the observations made with

Cases 1 and 2 configurations, the increase in ambient pressure makes the spray cone narrow, and that should have directed more droplets to the exit of the venturi rather than to the surface. But, in contrast, the VLIF imaging shows that droplets impinge more on the venturi at higher pressures and results in the formation of thicker rims.

The venturi acts as a confinement to the primary spray and the presence of venturi leads to the expansion of the primary spray at higher pressures. For the same air mass flow rate, the increase in density causes a proportional reduction in velocity, hence, the volume flow rate decreases. The bigger droplets of the primary spray impinge on the venturi wall and undergo wall filming. At lower air velocities and volume flow rates, and the spiralling time of the liquid film is more compared to the low-pressure case. The higher time scale of the film flow over the venturi surface results in thicker wall filming compared to the lower pressure cases. As a result, the accumulation time also increases, forming a thick liquid rim at the venturi.

**Effect of ambient pressure on rim breakup process**

The liquid rim accumulated at the venturi tip interacts with the counter-rotating shear layer formed by the interaction of the primary and secondary air streams. The internal flow field at the venturi exit is captured using the Case 4 configuration in which both primary and secondary swirler blocks are present. The internal flow field is visualized by the TR-VLIF imaging at an oblique angle [3] and the atomization process at the venturi exit is shown in Figure 9.

In the presence of secondary air also, a gradual increase in the rim thickness is observed at higher ambient pressures. Nevertheless, the proportional increase is not as prominent as observed in the venturi alone configuration, Case 3. At higher pressures, a dense droplet cloud is issued through the central region, along with the droplets generated from the liquid rim. Very fine droplets are observed at 1 bar compared to the bigger droplets and ligaments at 7 bar.

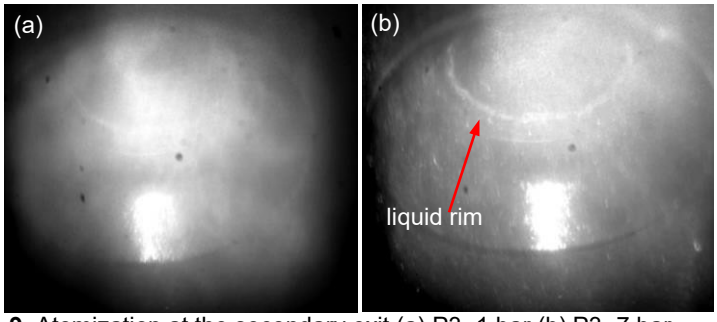


**Figure 9.** Atomization at the secondary exit (a) P3=1 bar (b) P3=7 bar.

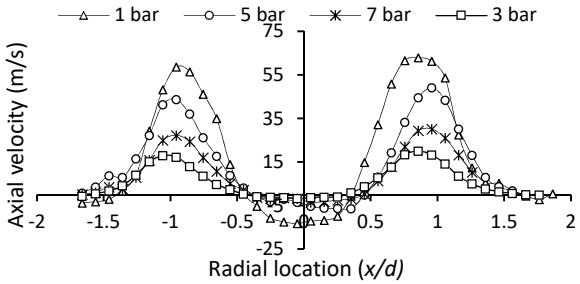


**Figure 10.** Velocity variation at the venturi exit in Case 4 at different P3 conditions (y/d = 1.43).

The axial velocity variation and SMD variation are shown in Figures 10 and 11 respectively. The secondary air improves the dominance of the air momentum and the recirculating flow field expands. As the P3 increases, the peak velocities at the spray cone

drops significantly (~55 to 17 m/s) and the recirculation zone contracts (-0.5 ≤ x/d ≤0.5), showing near-zero velocities in the central region. The droplet dispersion is affected by the air velocity field and bigger droplets are observed at higher pressures.

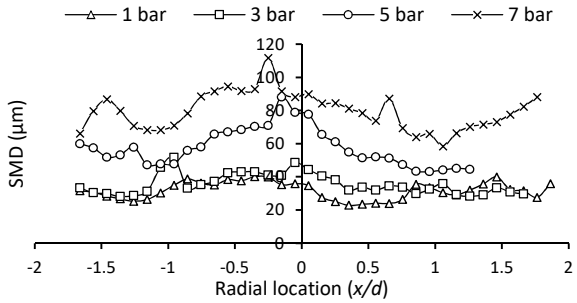


**Figure 11.** Diameter variation at the venturi exit in Case 4 at different P3 conditions (y/d = 1.43).

At the venturi exit, the droplet formation is mainly driven by two flow processes. In the central region, the atomization is influenced by the aerodynamic interaction of the primary air swirl and formation of CTRZ. The droplet size variation curve shows that in the central region, increase in the SMD is higher compared to the shear layer region, as the P3 increases. At the near field of venturi tip, the droplet formation occurs mainly by the breakup of the accumulated liquid rim in presence of the shear layer. The local circulation intensities at the shear layer region (±0.8 ≤ x/d ≤ ±1.1), accelerates the rim breakup [17] and a prompt atomization occurs within a very short distance from the venturi tip. This limits the influence of the ambient pressure on the drop formation in the shear layer region.

**Atomization at the swirl cup exit**

The spray structure at the swirl cup exit at 1 bar and 7 bar is shown in Figure 12. At P3=1 bar, the air momentum dominates the spray flow field and the droplet trajectories are dictated by the swirl flow field. The spray is also well atomized in this case. As the chamber pressure increases, the spray becomes denser with a slight expansion of the spray cone in the near field of the swirl cup exit. At 7 bar, bigger droplets are formed at the cup exit, and intermittently, large ligaments are shed into the central region.

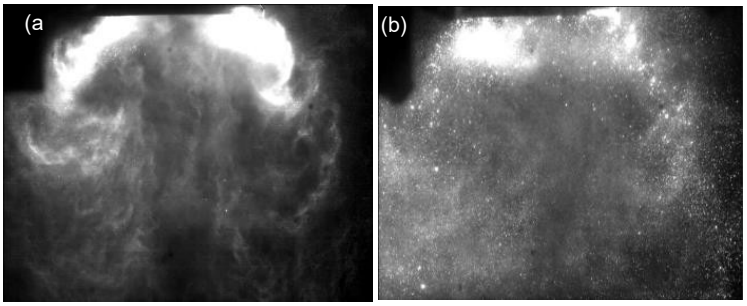


**Figure 12.** Instantaneous images showing the structure of the swirl cup spray at (a) P3 = 1 bar and (b) P3 = 7 bar.

The droplet size and velocity variation at different P3 values are shown in Figures 13 and14. The axial velocity at the shear layer region gradually decreases from 32-20 m/s as the chamber pressure increases. In the central region, the droplet velocity increases as the P3 increase, and this suggests that the droplet momentum is influencing the recirculating air flow. The droplet size variation shows that SMD increases as the chamber pressure increases showing a distinct trend in the central region (37-57 µm). However, it is important to note that the SMD is not increased considerably in the shear layer region. Overall, in the central region, bigger droplets are produced as the P3 increases, and this affects the velocity field also. The response of the swirl cup spray to the change in P3 is summarized in Figure 15. The average

SMD values are plotted against P3 for different stages. For the present test conditions, the pressure dependence of the average SMD can be expressed as follows:

$$\text{SMD} \sim P_3{}^m$$

Where,

m = 0.26 at primary exit (Case 2)
m = 0.5 venturi exit (Case 4)
m = 0.3 at swirl cup exit (Case 5)

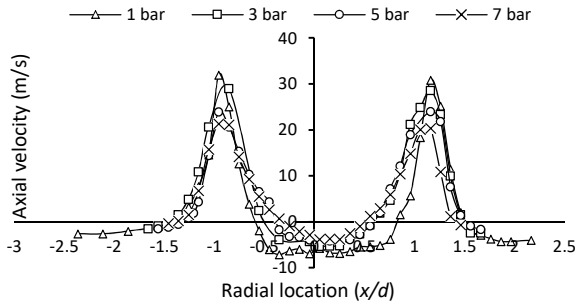


**Figure 13.** Velocity variation at the swirl cup exit at different P3 conditions (*y/d* = 1.7).

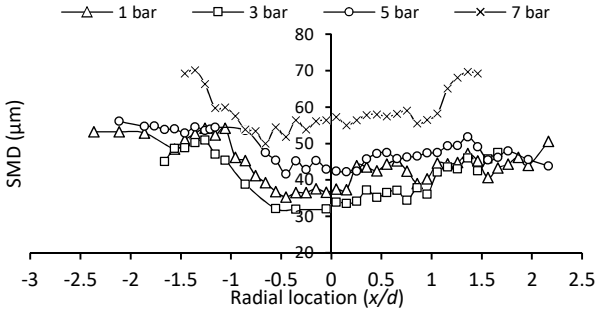


**Figure 14.** Diameter variation at the swirl cup exit at different P3 conditions (*y/d* = 1.7).

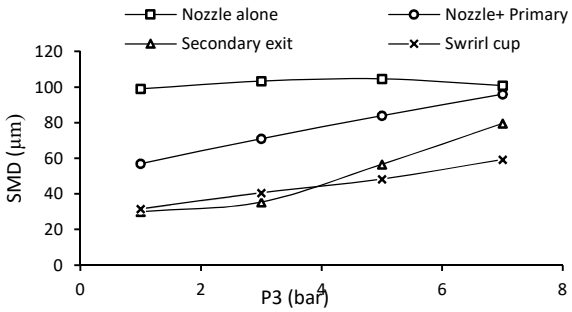


**Figure 15.** Variation of the average SMD with chamber pressure for different stage-wise configurations.

In general, the droplet size increases in all cases. As seen in the previous cases, a majority of the droplets in the centre region are originated directly from the pilot nozzle, and increase in the ambient pressure leads to the collapse of the pilot spray. These droplets undergo more aerodynamic interactions with the ambient air as they flow through the swirl cup and shows a higher response to pressure. Whereas, the atomization of the rim is mainly aided by the shear layer and the atomization completes within the immediate vicinity of the venturi tip, which is not much affected by the rise in P3. Hence, SMD is more influenced by the ambient pressure at the exit of venturi. Furthermore, the droplets generated within the shear layer are also present at the cup exit and the overall pressure dependence is reduced in this case.

## Conclusions

The present work investigates various internal atomization processes of the swirl cup at elevated pressure conditions using the stage-wise characterization approach. The internal two-phase flow evolution of the swirl cup is mainly decided by the pilot nozzle operation and the relative momentum exchange between the air and liquid.

The ambient pressure plays a significant role on the fuel placement inside the swirl cup and the droplet size distribution at the exit. The internal fuel placement at high pressures is dictated by the cone collapse of the primary spray and thick rim formation at the venturi tip. Nevertheless, the shear layer at the venturi exit limits the effects of pressure by effectively atomizing the rim within the near-field. At the venturi exit and at cup exit, the spray shows strong dependence on the ambient pressure particularly in the central region since the aerodynamic resistance of the primary air opposes the atomization in this region.

Counter-rotating shear layers are identified as an efficient atomization mechanism at high-pressure operating conditions. Injector designs can be improved by providing multiple coaxial air swirl circuits and fuel circuits rather than a single point injection by the pilot nozzle.

## Acknowledgements

The authors thank GE India Industrial Pvt. Ltd. for the financial support and also for providing the nozzle hardware for this investigation. The National Centre for Combustion Research and Development is supported by the Department of Science and Technology, India.

## Nomenclature

| | |
|---|---|
| *P3* | chamber pressure |
| *T3* | inlet air temperature |
| *ρ* | air density |
| *U(avg.)* | bulk air velocity |
| *Re* | Reynolds number |
| *SMD* | Sauter mean diameter |
| *ALR* | air to liquid ratio |
| *d* | venturi exit diameter |

## References

[1] Mongia HC, Al-Roub M, Danis A, Elliott-Lewis D, Jeng S, Johnson A, McDonell V, Samuelsen G, Vise S (2001), “Swirl cup modeling part 1” , 37th Joint Propulsion Conference and Exhibit, Salt Lake City, UT, USA, AIAA Paper 2001–3576.

[2] Lefebvre, A.H., 1998, Gas Turbine Combustion, Taylor & Francis, Philadelphia, USA, 2nd edition.

[3] Shanmugadas, K. P., Chakravarthy, S. R., Chiranthan, N., Jayanth Sekar, Sundar Krishnaswami, 2018, “Characterization of wall filming and atomization inside a gas turbine fuel injector”, Experiments in Fluids, Vol. 59, 151.

[4] Shanmugadas, K. P., Chakravarthy, S. R., 2017, “A canonical geometry to study wall filming and atomization in pre-filming coaxial swirl injectors”, Proceedings of the Combustion Institute, Vol. 36, pp. 2467-2474.

[5] Jasuja, A. K., Lefebvre, A. H., 1994, “Influence on ambient pressure on Drop-size and velocity distributions in dense sprays”, Proceedings of the Twenty-Fifth Symp. (Intl.) on Combustion, Combustion Institute, pp. 345-352.

[6] Zheng, Q. P., Jasuja, A. K., Lefebvre, A. H., 1997, “Structure of airblast sprays under high ambient pressure conditions”, Journal of Engineering for Gas Turbines and Power, Vol. 119, pp. 512-518.

[7] Jasuja, A. K., 1981, “Air blast atomization of alternative liquid petroleum fuels under high pressure conditions”, Journal of Engineering for Power, Vol. 103, pp. 514-518.
[8] McDonell, V. G., Seay, J. E., Samuelsen, S., 1994, “Characterisation of the non-reacting two-Phase Flow Downstream of an Aero-Engine Combustor Dome Operating at Realistic Conditions”, In: International gas turbine and aero engine congress and exposition, GT- 263-1994, Hague, Netherlands, 1994.
[9] Feras, Z. B., Roisman, I. V., Tropea, C., 2007, “Spray generated by an Airblast atomizer at high pressure conditions”, In: Proceedings of ASME Turbo Expo 2017: Power for Land, Sea and Air, ASME GT2007-27803, Montréal, Canada, 2007.
[10] Brandt, M., Rachner, M., Schmitz, G., 1998, “An experimental and numerical study of kerosene spray Evaporation in a Premix duct for gas turbine combustors at high pressure”, Combustion Science and Technology, Vol.138, pp. 313-348.
[11] Becker, J. Hassa, C., 2004, “Experimental Investigation of spatial and temporal aspects of the liquid fuel placement in a Swirl cup at elevated pressure”, In: Proceedings of ASME Turbo Expo 2004: Power for Land, Sea and Air, ASME GT2004-53524, Vienna, Austria, 2004.
[12] Jasuja, A. K., Lefebvre, A. H., 2001, “Influence of ambient air pressure on pressure-swirl atomizer spray characteristics”, ASME 2001-GT-0043.
[13] Shanmugadas, K. P., Chakravarthy, S. R., 2017, “Characterization of an aero engine fuel injector spray at realistic engine conditions”, Proceedings of the 1st National Aerospace Propulsion Conference, Kanpur, India.
[14] Shanmugadas, K. P., Chakravarthy, S. R., Chiranthan, N., Jayanth Sekar, Sundar Krishnaswami, 2018, “Spray characteristics of a dual orifice swirl cup at elevated pressures and temperatures”, 14th Triennial International Conference on Liquid Atomization and Spray Systems, ICLASS 2018, Chicago, USA.
[15] Gepperth, S., Koch, R., Bauer, H. J., 2013, “Analysis and comparison of primary droplet characteristics in the near field of a Prefilming airblast atomizer”, In: ASME Turbo Expo: Power for Land, Sea and Air, Volume 1A: Combustion, Fuels and Emissions, pp. V01AT04A002.
[16] Inamura, T., Shirota, M., Tsushima, M., Kato, M., Hamajima, S., Sato, A., 2012, “Spray characteristics of prefilming type of airblast atomizer”, 12th Triennial international conference on liquid atomization and spray systems, ICLASS 2012, Heidelberg, Germany.
[17] Rajamanickam, K., Basu, S., 2017, “On the dynamics of vortex– droplet interactions, dispersion and breakup in a coaxial swirling flow”, Journal of Fluid Mechanics, Vol. 827, pp.572-613.